The Journal of Phytopharmacology 2021; 10(1): 48-55
Online at: www.phytopharmajournal.com

Review Article

ISSN 2320-480X
JPHYTO 2021; 10(1): 48-55
January- February
Received: 25-11-2020
Accepted: 15-01-2021

doi: 10.31254/phyto.2021.10110

Tomer Sinai
Department of Biomedical Engineering, Ben Gurion University of the Negev, Be'er Sheva, Israel

Brijesh Singh
Department of Biochemistry and Pharmacology, Ben Gurion University of the Negev, Be'er Sheva, Israel

Amnon C Sintov
Department of Biomedical Engineering, Ben Gurion University of the Negev, Be'er Sheva, Israel

Shimon Ben-Shabat
Department of Biochemistry and Pharmacology, Ben Gurion University of the Negev, Be'er Sheva, Israel

Correspondence:
Prof Amnon C Sintov
Department of Biomedical Engineering, Ben Gurion University of the Negev, Be'er Sheva, Israel
Email: asintov@bgu.ac.il
Prof. Shimon Ben-Shabat
Department of Biochemistry and Pharmacology, Ben Gurion University of the Negev, Be'er Sheva, Israel
Email: sbs@bgu.ac.il

Synthesis, Isolation, and Biological Evaluation of a New Active Quinone Methide Derived Curcuminoid

Tomer Sinai, Brijesh Singh, Amnon C Sintov*, Shimon Ben-Shabat*

ABSTRACT

A new curcuminoid, quinone methide cyclopentadione (QMC), was synthesized by oxidation of curcumin (CUR) in the presence of potassium ferricyanide, and further isolated and analyzed. QMC was found to be a relatively water-soluble curcuminoid, and more stable than CUR in citric-phosphate buffer solutions. Unlike CUR, QMC possesses a pH-independent stability. In plasma, QMC was degraded by 50% after 8 hours and reached 30% of its initial concentration after 48h, while CUR was thoroughly decomposed. It has been demonstrated that QMC has a similar anti-proliferative activity as CUR in three different cancer cell lines- MCF-7, PC3 and HT29. Molecular examination of QMC in cancer cells exhibited similar effect to CUR on two transcription factors, Nrf-2 and NF-κB. An anti-inflammatory activity of QMC was demonstrated by measuring MCP-1 secretion levels in TNFα-induced human keratinocytes cell culture, which had been pre-treated with either CUR or QMC. This report presents the advantages of the new quinone methide derived curcuminoid and its pharmaceutical potential as an alternative to the poorly soluble curcumin.

Keywords: Curcumin; Quinone methide cyclopentadione; Cell proliferation; Anti-inflammatory activity; Oxidation.

INTRODUCTION

Curcumin is the major yellow pigment extracted from turmeric, a spice that is used in Ayurvedic herbal remedies [1, 2]. It is a potential and promising active agent with a variety of pharmacological activities, such as an anti-inflammatory effect in Crohn's disease, ulcerative colitis, rheumatoid arthritis, psoriasis, peptic and gastric ulcer, as well as a therapeutic activity for breast, skin, oral and intestinal cancers, microbial and viral infections and diabetes, just to name a few [1-4]. The anti-inflammatory effects of CUR are associated with inhibition of pro-inflammatory chemokines, reduction of neutrophil and macrophage infiltration, as well as suppression of COX-2, IL-8 and other proinflammatory targets in-vivo and in vitro [5-7]. In psoriasis, which is an immune-mediated skin inflammation disease, the beneficial role of CUR was validated in several human and animal studies [8-10]. CUR molecule is an a bis-a,b unsaturated b-diketone that exists in equilibrium with its enol tautomer (Figure 1). Under alkaline condition, the enolate form is predominant while the bis-keto form predominates in acidic and neutral aqueous solutions due to the highly activated carbon atom in the heptadienone linkage between the two methoxyphenol rings [11]. Tønnensen and Karlsen found that CUR in aqueous solutions (containing also methanol) at pH 1-7 is in the neutral state exhibiting yellow color, which changes to red color when pH decreased to <1 (protonated form) or increased to pH>7.5 (enolic form with a pKa of approximately 7.8, and two phenolic protons with pKa values of 8.55 and 9.05 [12]. CUR is not chemically stable at physiological solutions, as 90% decomposed within 30 min when incubated in serum-free phosphate buffer, pH 7.2 [13]. According to that study, the major degradation product was *trans*-6-(4'-hydroxy-3'-methoxyphenyl)-2,4-dioxo-5-hexanal, and minor products were found to be vanillin, ferulic acid, and feruloyl methane. Due to CUR's rapid metabolic transformation, it is hypothesized that the observed pharmacological effects are not caused by CUR itself but are due to its metabolites [14-16]. The *in vivo* metabolism involves stepwise reduction in the gut by the NADPH-dependent reductase CurA from intestinal E. coli, and alcohol dehydrogenase [17] reduces CUR to tetra- and hexahydro-curcumin in the liver [18-20]. The main metabolites detected in the plasma are those mediated by sulfation and glucuronidation of CUR and its tetrahydro/hexahydro metabolites (reductive metabolites). However, these detectable metabolites have been found to be biologically inactive or at least less active than CUR [21]. In a recent study, the most prevalent product of CUR degradation was identified as the one formed by autoxidative transformation, bicyclopentadione [22-23]. It has also been suggested that the hydrolysis pathway is limited and has a minor contribution to CUR degradation, compared to the autoxidative route. Although the researchers have demonstrated that bicyclopentadione can also be enzymatically formed via LOX-1 purified from soybean [24] and purified recombinant human COX-2 [22], there is no evidence that this conversion happens *in vivo* [23]. Furthermore, Sanidad *et al*. [25] have shown that total degradation products of CUR and isolated bicyclopentadione had a decreased anti-inflammatory effect compared to their parent agent in MC38 colon cancer cells and in RAW 264.7 macrophage cells. It has also been shown

that when CUR degradation had been suppressed (by redox active antioxidants), its biological activities were enhanced [26] This implies that the oxidative degradation products cannot play a major role in CUR activity, while another metabolite (or metabolites) formed in cells is the real mediator of CUR effects. Apart of its rapid degradation and metabolism as well as the unclear mechanism of action, CUR is poorly soluble, slightly absorbed into the body with a very low bioavailability [16]. It is of crucial importance, therefore, to seek other pathways of CUR degradation that might formed and take part in eliciting the biological effects. In our study, we have isolated and characterized a new oxidative degradation product of CUR and evaluated its biological activity. $K_3[Fe(CN)_6]$ was chosen as an oxidizing reagent following previous publication demonstrating its activity in oxidation of organic compounds [23, 27]. By reacting this oxidant with CUR, we obtained a compound identified as (E)-4-(2-hydroxy-5-(4-hydroxy-3-methoxybenzoyl)-4-oxocyclopent-2-eny1idene)-2-methoxycyclohexa-2,5-dienone [QMC; Quinone Methide Cyclopentadione] (Figure 1). QMC is a partially conjugated organic molecule having almost the same molecular weight as CUR (MW=368.139 Da). By comparing with CUR, QMC has a different structure and chemical nature, it is soluble in aqueous solutions, and it has similar anti-proliferative activities as CUR in malignant cancer cells. To have a better perspective of QMC anti-cancer activity, we examined (*in-vitro* and *in-silico*) the translation factors Nrf2 and NF-κB, two signalling proteins involved in cancer activity known as being altered by CUR [28-31]. To estimate the anti-inflammatory effect of QMC in comparison with CUR, we used the TNF-α induced inflammation model of HaCaT cell-line, which is a well-known *in vitro* cell culture model of psoriasis [32-34].

METHODS

CUR oxidation and QMC isolation

Synthesis

A solution of 100mM Tris-HCl buffer pH 8 was prepared by dissolving 12 g of tris(hydroxymethyl)aminomethane (Sigma-Aldrich, Rehovot, Israel) in 900 mL purified water, then the solution was acidified with 10N HCl solution and made up to 1L. CUR (Chem-Impex, Wood Dale, IL)) was dissolved in methanol to obtain a 1 mg/mL solution. Potassium ferricyanide (Merck&Co., Darmstadt, Germany) was dissolved in the Tris buffer at a concentration of 0.05M. In a 500 mL round bottom flask, 60 mL of 1 mg/mL CUR in methanol solution were diluted to a concentration of 0.325mM in 500mL of 100 mM Tris-HCl buffer pH 8. The reaction was allowed to stir for 3 days while aliquots of 210µL of 0.05M $K_3[Fe(CN)_6]$ solution were added daily. After 72h the solution was acidified to pH 6 with 1N HCl solution and then washed 3 times with 150mL ethyl acetate to extract the organic products. The organic solution was concentrated under vacuum and then injected to semi-preparative HPLC column for separation. Ethyl acetate, methanol, and hydrochloric acid were purchased from BioLab, Israel.

Product Isolation and Characterization:

The extracted reaction mixture was separated by a high-pressure liquid chromatography system (Varian ProStar, USA) equipped with a prepacked C_{18} column (Betasil C18, 5µm, 250×4.6 mm, ThermoHypersil, UK) and a diode array detector. The samples were eluted by a gradient of 20% to 80% acetonitrile in a 0.02% aqueous acetic acid solution over 30 min at a flow rate of 1 mL/min and peaks were detected at 380nm. Isolation and collection of QMC were conducted by the same HPLC system, equipped with a semi-preparative C_{18} column at a flow rate of 4.5 mL/min. After several running procedures, the collected samples were dried under vacuum. HPLC grade solvents were obtained from J.T. Baker (Mallinckrodt Baker, Inc., Phillipsburg, NJ). Structure elucidation was carried out using a nuclear magnetic resonance (NMR) and mass spectrometry (LC-MS system: HPLC Agilent 1100 Series connected to UV detector & ion trap MS Esquire 3000 Plus Bruker Daltonics detector equipped with Electro-Spray; MS Orbitrap system: Thermo-Fischer LTQ XL Orbitrap with nano-ES capillaries). ^{1}H NMR spectra were (Figure 1-S, Table 1-S) recorded on a Bruker DMX-500 operating at 500.1 MHz, and chemical shifts were reported in ppm. ^{1}H-NMR (CD3OD): 7.49**-**7.45 (d, 2H), 7.3 (s, 1H), 7.00 (d, 1H) 6.95-6.97 (d, 1H), 6.72 (m, 1H), 6.00 (s, 1H), 4.08 (s, 3H), 4.03 (s, 1H), 3.90 (s, 3H), LC-ESI-MS (positive QMCe): m/z _368.9 $[M+H]^+$. MS orbitrap analysis (Elemental analysis) of the compound (Figure 2-S) showed a mass of 369.0969 m/z (369.098 m/z calculated mass of $[C_{20}H_{16}O_6^+]H^+$). MS/MS (Figure 3-S; Positive QMCe): m/z 350.9; 322.9; 244.9; 190.9; 177; 123 (Figure 2B).

Cell Cultures

Human keratinocyte (HaCaT) cell line, MCF-7 (human breast adenocarcinoma) and PC-3 (human prostate cancer) cells were cultured in Dulbecco's Modified Eagle's medium (DMEM) and DMEM/F12 containing 10% fetal calf serum, 5% L-glutamine and 5% penicillin/streptomycin. HT29 cells (Human colon epithelial cells from colorectal adenocarcinoma) were cultured in McCoy's Modified Medium containing 10% fetal calf serum, 5% L-glutamine and 5% penicillin/streptomycin. All cell types were maintained at 37˚C in a humidified atmosphere of 95% air and 5% CO_2. The medium was refreshed every 2–3 days and when the cells reached 90% confluence, they were either experimentally seeded or sub-cultured in a 1:10 dilution using trypsin-EDTA. Growth media and supplements were supplied by Biological Industries Ltd. (Kibbutz Beit Ha'emek, Israel).

Cell proliferation experiments

All three cell lines were seeded in a 96-well plate ($5x10^3$ cells per well) after counted by a glass hemocytometer. Weighed samples of QMC and CUR were dissolved in DMSO at a concentration of 25mg/mL solutions. Twenty-four hours after seeding, various volumes of these solutions were added paying attention to not exceeding 0.9% DMSO per well. 24 and 48 hours after treatments, the growth media were removed, and the cells were washed twice with PBS solution. After removing the PBS solution, volumes of 100mL growth media were added to each well with 50mL of pre-activated XTT solution (2,3-bis-(2-methoxy-4-nitro-5-sulfophenyl)-2H-tetrazolium-5-carboxanilide, Biological Industries Ltd., Kibbutz Beit Ha'emek, Israel). After incubation at 37°C in a 5% CO_2 atmosphere for 4 hours, each plate was scanned by ELISA reader at 450nm (Sunrise™, Tecan Group Ltd., Männedorf, Switzerland).

Cell inflammation experiments

Cultured HaCaT cells ($1x10^6$ cells in single culture dish) were treated with 20µM of QMC, CUR, calcitriol (Vitamin D_3) and calcipotriol (all dissolved in DMSO). Calcipotriol (or calcipotriene) was provided by Teva Pharmaceutical Industries Ltd. (Kfar Saba, Israel), and calcitriol was obtained from Sigma-Aldrich (Rehovot, Israel). After 6-hour incubation, the culture media with the different treatments were replaced by a TNFα–containing medium (10ng/mL), or a standard medium (control) for further 24-hour incubation (37˚C in a humidified atmosphere of 95% air and 5% CO_2). The culture media were collected

in pre-chilled vials, centrifuged at 1000g for 15min and analyzed for MCP-1 by an ELISA assay kit (Biolegend, San Diego, CA).

Western Blot Analysis

MCF7 cells were seeded in 6-wells plates ($0.6x10^6$ cells per well) and incubated at 37°C in a 5% CO2 humidified atmosphere. After 24h, the medium was replaced with a fresh medium containing either 20µM QMC or CUR. 24h after treatment, cell lysis was carried out in an ice-cold RIPA buffer (50mM Tris buffer solution, pH 7.4, 150mM NaCl, 1mM EDTA, 1% Triton X-100, 1% deoxycholate, 0.1% SDS, 1mM dithiothreitol and 10µl/mL protease inhibitor cocktail). Protein concentrations were determined using the Bradford protein assay (Bio-Rad Laboratories Ltd., Rishon Le Zion, Israel). The proteins from each sample (30µg of protein) were separated by 10% SDS-polyacrylamide gel electrophoresis (SDS-PAGE), then transferred to a nitrocellulose membrane (Pall Corporation, Port Washington, NY). Each membrane was blocked in TBST buffer (10mM Tris buffer solution, pH 7.5, 100mM NaCl and 0.05% Tween 20) containing 3% non-fat dried milk. The blots were probed with primary antibodies overnight (ab137550, anti-NRF2 from ABCAM 1:500 dilution; sc-8008, anti-NF-κB from SCBT 1:1000 dilution; ICN691001, anti-actin from MP Biochemicals, 1:5000 dilution) followed by 2h exposure to secondary antibodies (Cells Signalling Technology anti-rabbit IgG HRP-linked antibody or antimouse Jackson Immuno Research). The blots were then developed and visualized with the enhanced chemiluminescent EZ-ECL Detection kit for HRP (Biological Industries, Kibbutz Beit-Haemek, Israel) on an ImageQuant LAS 4000 digital imaging system (General Electric Healthcare Bio-Sciences, Pittsburgh, PA).

***In-silico* analysis**

The binding interactions of QMC and CUR with Keap-1 and NF-κB p50 proteins were simulated using AutoDock Vina software. ACD/Chem-Sketch (Freeware) were used to draw 2D structure of CUR and QMC after converted to 3D structure in MDL molfiles format. From the Protein Data Bank (http://www.rcsb.org/pdb), X-ray crystal structure of keap1 complexed with IQK ligand (PDB ID: 4IQK) and NF-κB p50 dimer complexed with DNA (PDB ID: 1NFK) were obtained. Using Discovery studio visualizer V.17.2.0, keap1 chain -A was selected and saved in PDB format while deleting the bound IQK ligand, opening the PDB file in text format and removing water and ions as hetero-atoms. Calculated Gastegier charges of keap1 subunit were saved in PDBQT file format using AutoDock Vina. AutoDock Vina grid box for docking was defined based on a known binding site in protein macromolecule [35]. Grid box size of 80×42×46Å with 0.375Å spacing was used to include IQK ligand binding residues. Docking to protein was done based on hybrid energy function (empirical + knowledge-based). Using Discovery studio visualizer V.17.2.0, NF-κB p50 chain A was selected and saved in PDB format while deleting the bound DNA. After removing water and ions as hetero-atoms, Gastegier charges to NF-κB p50 subunit were calculated and saved in PDBQT file format using AutoDock Vina. Using AutoDock Vina, grid box of size of 46×82×112 Å with 0.375Å spacing was used, including DNA binding residues based on known binding site with CUR [36]. Docking to protein was done based on hybrid energy function (empirical + knowledge-based). Protein–ligand complex for lowest free energy of binding (delta G) confirmation was written and saved in form of log file.

Stability and Solubility testing of QMC and CUR

Stability in aqueous medium: To evaluate the stability of QMC and CUR in a buffer solution at various pH values, 100mM Na_2HPO_4 (Sigma-Aldrich, Rehovot, Israel) and 200mM Citric acid solutions in DDW were mixed together at different ratios to produce buffers of pH 3.0, 7.4, and 8.0. Buffer solution at pH 9 was obtained by adding an appropriate volume of 0.5M NaOH solution to 100mM Na_2HPO_4 solution. The stability analysis was performed as previously described [13, 37]. CUR or QMC solutions (1mg/mL) in methanol were diluted to 50mg/mL with buffer solutions (in triplicate for each pH) and incubated at 25ºC (in a controlled climate chamber), during which samples were taken at t=0, 8, and 24h. Samples were extracted twice by equal volumes of ethyl acetate and the collected organic solvent was evaporated to dryness. The residue was re-dissolved in methanol and kept at 4°C until analyzed by HPLC.

Stability in rat plasma: CUR solution (1mg/mL) in methanol was diluted to 50mg/mL concentration with rat plasma. QMC was weighed and directly dissolved in rat plasma to get a 50mg/mL concentration. The plasma specimens were incubated at 37ºC (in a controlled climate chamber), and were sampled every one hour for 8 hours, then sampled at 24h and 48h. The samples were diluted with two volumes of methanol and centrifuged at 13,000g for 10 min at 4ºC, and the supernatant was then collected. The methanolic solutions were injected into an HPLC for analysis against a standard calibration curve.

Aqueous solubility: the test was preform as described by Ramya *et al*. [38]. Triplicates of 1mg samples of CUR or QMC were added to 2.0 mL of HPLC grade water. The samples were vortexed for 5 min, sonicated for 5 more minutes, and incubated with constant stirring at 37°C for 24h. The mixtures were then centrifuged at 14,000 rpm for 15 min and the supernatant solution was quantified for CUR or QMC by HPLC analysis.

RESULTS

QMC is a water-soluble oxidation product of CUR

As a result of 72-h reaction with potassium ferricyanide [$K_3Fe(CN)_6$], several degradation products of CUR were detected. The reaction mixture was then divided to fractions which were screened for their anti-proliferative activity in MCF-7 cells. Further screening was performed for compounds isolated from the active fraction, brought about the discovery of an active anti-proliferative component. NMR and MS analyses of this isolated active compound have indicated that the new substance, abbreviated QMC, has an unprecedented structure of curcuminoid with methoxy phenol groups, quinone methide moiety and a cyclopenatdione (Figure 1). The oxidation of phenols to quinone methides by $K_3Fe(CN)_6$ has already been studied previously (Krysin *et al*., 2014), showing to create a potential electrophile for a Michael addition reaction. An indication of a quinone group in QMC molecule was observed by NMR spectrum, following a chemical shift at 6.95-7.00 ppm (Table 1-S). Mass spectrum measurements were carried out using a prototype Orbitrap mass spectrometer, showing m/z of 369.0969 by using a simple one-point calibration, which was in a good agreement with the calculated mass of 369.0980 (Figure 2-S). The mass accuracy of this measurement was 1.0 ppm. Purified QMC exists as two tautomeric isomers which can be separated by reverse phase HPLC (Figure 2) after isolation from the organic extract of the reaction. Attempts to oxidize CUR quantitatively in shorter time periods than 72h had failed. It is also important to note that QMC could not be

created by auto-oxidation reaction, and it would not be formed without the addition of an oxidizing reagent.

QMC solubility and stability in physiological pH and plasma.

Relative to the practically water insoluble CUR (<0.1mg/mL), QMC solubility was as high as 0.8mg/mL. QMC is more stable than CUR for 24h in physiological pH buffers (Figure 3A, 3B). In rat plasma, QMC metabolized by 50% in the first 5-6 hours, followed by a slow degradation rate which leaving 20%-40% of intact compound after 24h and 48h. CUR was apparently more stable in plasma and degraded by about 30% in 24h, but was completely worn off after 48h (Figure 3C).

QMC inhibits cancer cell lines proliferation

To evaluate the anti-cancer activity of QMC relative to CUR, XTT proliferation assays were carried out for 24 and 48 hours with three human cancer cell lines, MCF7, HT29, and PC3, which their growth has been previously shown to be inhibited by CUR [39-41] (Figure 4). In the present study, we have demonstrated that both CUR and QMC significantly inhibited cell growth at concentrations of ≥5μM. It has also been shown that QMC was more potent as an anti-proliferative agent than CUR, particularly in PC3 cell culture. The higher potency of QMC relative to CUR was more notable after 48-h treatment. The 48-h treatment with QMC demonstrated that even at a low concentration of 0.5μM, the cancer cells proliferation was suppressed.

QMC inhibition activity involves reduction in NF-κB and elevation in Nrf2 protein levels.

Nrf2, is ubiquitously expressed in various tissues as a transcriptional activator for phase II genes by binding to Antioxidant Responsive Element (ARE) sequences. Nrf2 activation depends on Keap1 (Kelch ECH Associating Protein 1), a cytoskeleton protein capable of binding to actin filaments and Nrf2, thus inhibiting its nuclear translocation and acting as a repressor during basal conditions [42]. Under oxidative stress, Nrf2 is released from Keap1 repression, translocated to the nucleus, forms heterodimer with small Maf (musculoaponeurotic fibrosarcoma) proteins in order to bind to cis-acting ARE, afterwards it ignites assembly of the whole transcription machinery including the RNA polymerase II to transcribe its target genes. Consequently, Nrf2 is a master regulator of cellular antioxidant and cytoprotective defence systems that protects humans from genotoxic damage caused by carcinogens. In-vivo studies in Nrf2-null mice have established the essential role of Nrf2 in cancer protection [42-44]. Another signalling pathway involves cancer pathogenesis and progression is the NF-κB pathway. The activation of NF-κB pathways takes part in the tumorigenesis process by transactivating target genes that have immunoregulatory, inflammatory, anti-apoptotic, and cell cycle regulatory functions [44]. Cross-talk between these pathways (Figure 5[I]) are in inverse relationship, as Nrf-2 activation induces intracellular events that causes NF-κB suppression and vice versa [44-46]. The elevation of Nrf2 after treatment of breast cancer cell line by CUR has been previously studied [31], and it involved a decrease in Fen1 (Flap endonuclease1) activity. It has also been shown that the anti-cancer activity of CUR involves disruption of the NF-κB pathway in several cancer cell lines [47-48]. In our study we have found that the anti-cancer mechanism of both QMC and CUR was connected to elevation in Nrf2 and to decrease in NF-κB protein level (Figure 5[II]), demonstrating that QMC and CUR share similar activities.

***In-silico* analysis reveals that QMC binds to NF-κB p50 subunit and Nrf-2 suppressor Keap-1.**

Keap-1 is an inhibitor complex that suppresses Nrf-2 from being released in the cytoplasm and translocate to the nucleus. Interaction between Keap-1 subunit and CUR had been demonstrated in previous studies [35, 49-50], therefore we examined QMC and CUR binding to Keap-1 by docking studies using AutoDock Vina software (Figure 6A). As summarized in Table 1, CUR bound to keap1 subunit with ΔG of -8.4 kcal/mol. The hydroxyl group and oxygen atom of methoxy group (-OCH_3) group of CUR forms hydrogen bonding with SER508 and ARG483. ALA556 depicts pi alkyl interaction. GLY 603 and GLY 364 forms hydrogen bonding with hydroxyl group. GLY509 shows Van der Waals interaction. VAL606 forms hydrogen bonding with oxygen atom of methoxy group. QMC bound to Keap1 subunit with ΔG of -9.2 kcal/mol (Table 1). The hydroxyl group of QMC forms hydrogen bonding with ASN414, ARG415, GLN530, GLY462, GLY509, TYR334 and TYR525. Hydrophobic interaction of type pi-pi has been found between QMC, TYR572 and ALA556.SER508 and GLY364 forms hydrogen bonding with oxygen atom of methoxy group (-OCH_3). SER602 forms hydrogen bonding with QMC's carbonyl group (Figure 6A). Suppression of the NF-κB transcription factor protein complex is linked to CUR's ability to bind to the p50 subunit [36, 49]. Inhibition of the NF-κB p50 subunit by CUR and QMC showed (Figure 6B) that CUR bounds to p50 with ΔG of -6.7 kcal/mol, while QMC bound to NF-κB p50 subunit with ΔG of -7.8 kcal/mol (Table 1). The hydroxyl group and the oxygen atom of methoxy group (-OCH3) of CUR formed hydrogen bonding with GLY52 and GLY65, respectively. ASN 136 depicts conventional hydrogen bonding with the hydroxyl group of CUR. The hydroxyl group of QMC forms hydrogen bonding with SER63 and ASN136. Hydrophobic interaction of type pi-pi has been found between QMC and PHE53, while Pi-Alkyl type of interaction has been found between the compound and PRO68 with LYS77 (Figure 6B).

Table 1: Binding site amino acids interactions and ΔG of QMC and CUR at Keap-1 and NF-κB p50 proteins.

Protein	Compound	Binding ΔG (kcal/mol)	Amino Acids at binding site
Keap-1	CUR	-8.4	ARG 483, SER508,GLY509, GLY603,GLY364,VAL 606,ALA 556
	QMC	-9.2	ASN 414, ARG415, GLN530, GLY462, GLY509, TYR334 and TYR525
NF-κB p50	CUR	-6.7	GLY52, GLY65 and ASN136
	QMC	-7.8	SER63, PHE53, PRO68, LYS77, ASN136

QMC reduce MCP-1 secretion in TNFα- induced HaCaT cells.

Monocyte chemoattractant protein 1 (MCP-1) is a pro-inflammatory cytokine that is secreted during inflammation of various types of tissues, including the skin [34, 51]. To evaluate the anti-inflammatory effect of QMC on skin cells, cell culture media samples of 24-h TNFα-induced HaCaT cells pre-treated with 20µM of either QMC, CUR, calcitriol or calcipotriol were collected and measured for their MCP-1 levels. Calcitriol is an active form of vitamin D and calcipotriol is a vitamin D derivative, both compounds are commercially used as anti-inflammatory medications for skin disease [52]. It has been shown previously [32-33] that CUR effectively reduces inflammation in HaCaT cells within several hours. Similar to CUR (Figure 7), QMC significantly down-regulated MCP-1 levels after 6h, compared to calcitriol, calcipotriol and untreated TNFα induced cells.

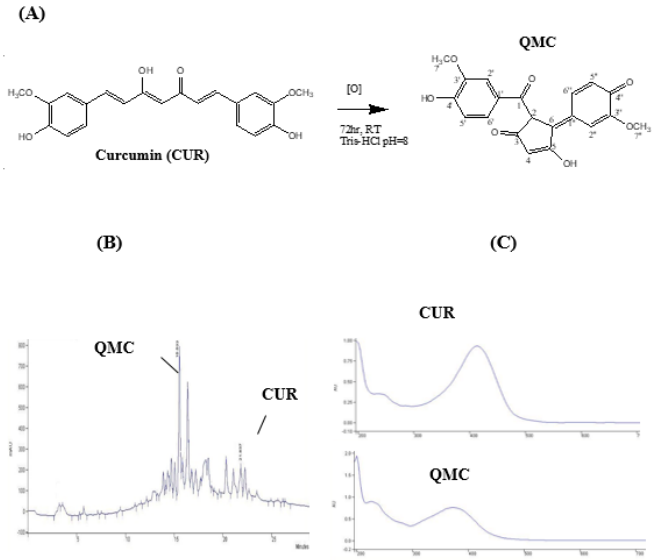

Figure 1: Oxidation of CUR with potassium ferricyanide for 72h in Tris buffer. QMC was formed as the main degradation product of CUR (A), followed up by HPLC analysis at λ=380nm (B). QMC has a distinct shift towards 380nm in a visible light absorbance, as seen in the spectrum of both compounds by UV/Vis HPLC detection (C).

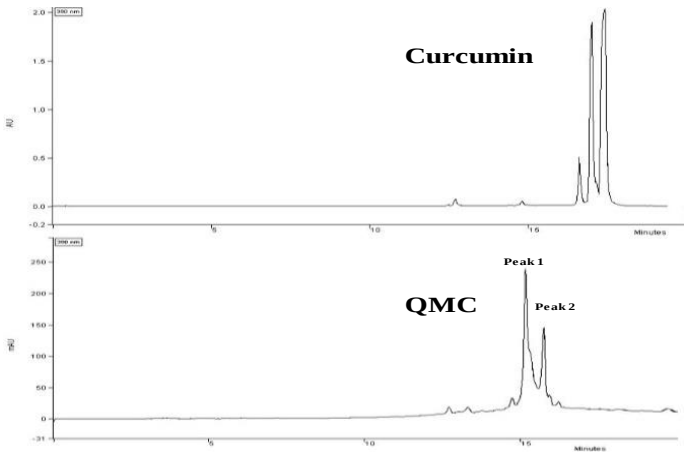

Figure 2: (A) Pure QMC represented by two isomers as chromatographed by HPLC,

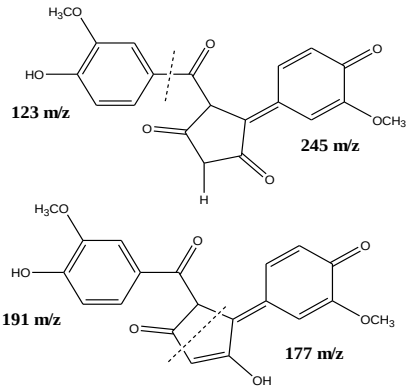

Figure 2: (B) the keto-enol tautomerization.

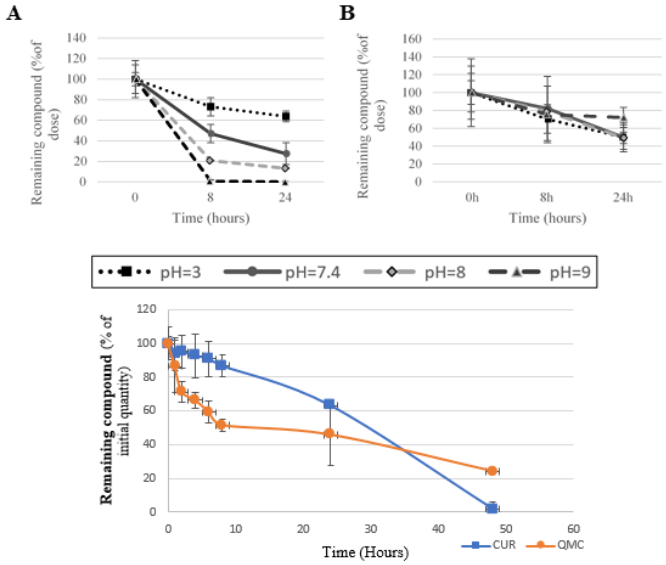

Figure 3: Stability of CUR (A) and QMC (B) (50mg/mL) during 24-h incubation at different pH values (citric-phosphate buffers), and in rat plasma (C). Data are presented as average ± SD; n=3.

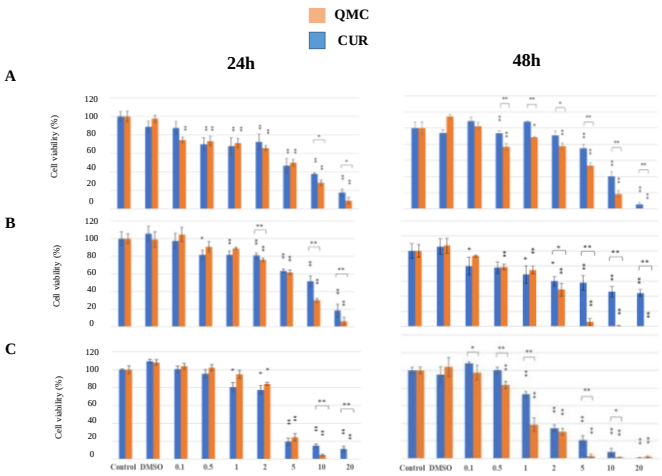

Figure 4: CUR and its oxidative product, QMC, have similar antiproliferative effects in cancer cell lines. (A) MCF-7 cells, (B) PC-3 cells and (C) HT-29 cells were untreated or treated with CUR, QMC or DMSO vehicle (0.1%) in DMEM (MCF-7 and PC-3) or McCoy's 5A Medium (HT-29) for 24−48 h. Cell proliferation was assessed by XTT assay. Results are expressed as percent of cell viability of compound-treated cells to non-treated cells, expressed as the mean ± SD (n=6, One-way ANOVA was used to determine statistical difference). (∗) P < 0.05 (∗∗) < 0.01.

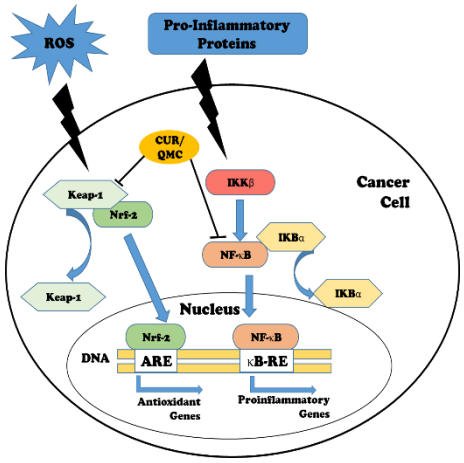

Figure 5: [**I**] Cross-signalling between NF-κB and Nrf-2 cancer: Inflammation generates oxidative stress and the other way around. Inflammation causes activation and nuclear localization of NF-κB after its detachment from IκBα, where it connects to κB response elements, inducing transcription pro-inflammatory proteins. Activation and nuclear localization of Nrf-2 after its release from Keap1 leads to Nrf-2 binding to the antioxidant response elements in the DNA and transcription of antioxidant genes. NF-κB signalling inhibits Nrf-2 signalling and vice versa. QMC elevates Nrf-2 levels and decreases NF-κB levels in the cytoplasm, possibly in a similar way CUR, by inhibiting Keap-1 and binding directly to NF-κB.

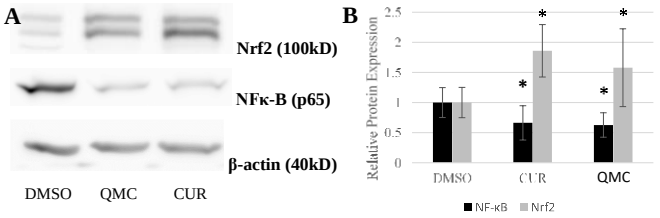

Figure 5: [**II**] Nrf2 and NF-κB proteins levels in MCF7 cells normalized to β-Actin (40 KD) in WB analysis after 24 hrs treatment of 20 CUR or QMC. (A) Representative Western blot film. (B) A significant increase in Nrf2 and decrease in NF-κB levels following either QMC or CUR treatments in comparison with DMSO (vehicle control). The bar graph represents the means ± S.D n=6. One-way ANOVA was used to determine statistical difference, as indicated by asterisks (*P < 0.05).

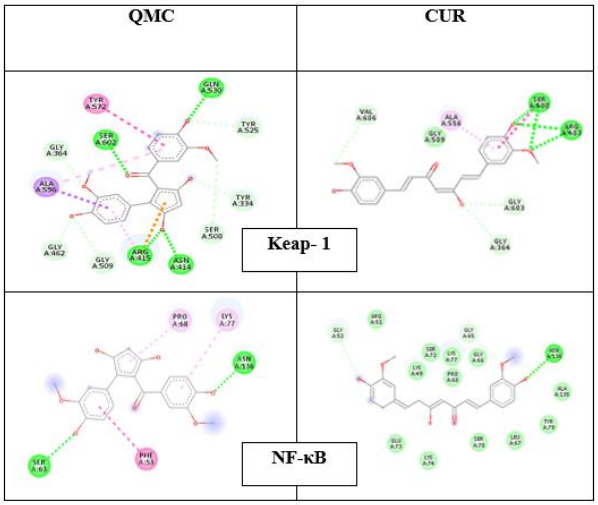

Figure 6: Schematic representation of the binding site of QMC and CUR to the catalytic site of Keap1 and NF-κB p50 subunit.

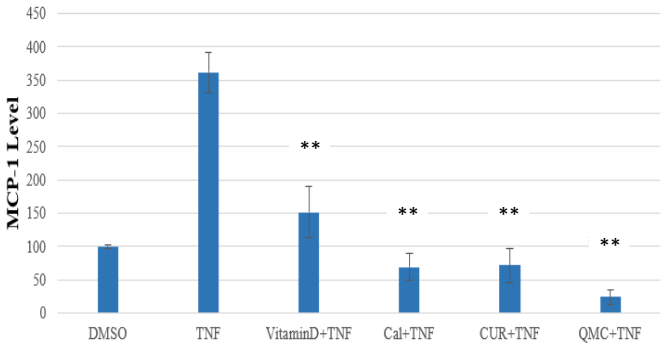

Figure 7: Culture media concentration of MCP-1 after 6-h pre-treatment with calcitriol (Vitamin D_3), calcipotriol (Cal), QMC and CUR followed by 24-hour treatment of TNFα. Six hours XTT evaluation of HaCaT cells with QMC\CUR showed no decrease in viability (data not shown). The bar graph represents the means of three separate experiments. One-way ANOVA was used to determine statistical difference, as indicated by asterisks (*P < 0.05).

DISCUSSION

CUR can potentially provide treatment for several pathologies such as cancer, inflammation and neurodegenerative diseases, however, its poor bioavailability, poor absorption, high systemic elimination rate and rapid metabolism limit its therapeutic use [2, 15-16]. CUR degradation in physiological solutions, with or without the presence of oxidants, results in products such as bicyclopentadione, vanillin, and ferulic acid [20, 22]. Several studies have demonstrated that these products are less likely to mediate CUR biological effects since they are less active [21, 25]. A recent study by Edwards *et al*. [53], indirectly showed that CUR has an anti-inflammatory activity due to an intermediate product formed by oxidation, seemingly a product containing quinone methide moiety. QMC, which contains a quinone methide group, was synthesized by our group using a modified oxidative degradation protocol of CUR in the presence of potassium ferricyanide. The cyclopenatdione formed in the QMC molecule could be generated from an intermolecular cycloaddition reaction. It is presumed that QMC was formed by a mechanism involving oxidation of one methoxy phenol groups into a quinone radical, as described previously [27], followed by intermolecular cycloaddition (Scheme 1). As shown in Scheme 1, the intermediate cyclopentadione product is coupled with reactive oxygen radical and undergoes aryl migration, followed by elimination of the alkyl oxide and further oxidation. This mechanism is based on prior studies of radical aryl migration and cycloaddition reactions in polyphenols [54]. Evaluation of the anti-cancer proliferation activity of QMC showed similarity to the CUR effect on several cancer cell lines. Since CUR has numerous protein signalling targets in cancer cells [55], we have chosen to find out whether QMC has a similar effect as CUR on the transcription factors Nrf-2 and NF-κB. These proteins crosstalk with each other and involved in cancer cellular signalling [44-46]. As previously shown, CUR upregulates Nrf-2 and downregulates NF-κB in cancer and other pathologies [48-49, 55]. The same effect as CUR on these proteins has been demonstrated by QMC in MCF-7 cells. It was, therefore, interesting to get more insight into the inhibitory mechanisms of CUR and QMC by using *in-silico* modelling. Since previous studies have shown that CUR directly inhibits the Nrf-2-suppersor Keap-1 [35, 49-50] and NF-κB p50 subunit [36], we calculated the protein-inhibitor free energy of QMC and CUR binding to these proteins. The similar binding affinity of the two compounds further explains the effect of QMC on Nrf-2 and NF-κB levels in MCF-7 cells, considering that Keap-1 inhibition upregulates Nrf-2 and the p50 subunit of NF-κB activity is essential for NF-κB assembly and DNA binding [56]. The anti-

inflammatory effect of CUR in various disease has been well established [2, 5]. In our study we examined the effect of QMC pre-treatment on TNFα-induced HaCaT keratinocytes, and compered it with CUR and two other positive control materials, calcipotriol (used topically for psoriasis) and calcitriol (vitamin D_3). Pre-treatment for 6 hours caused a dramatic decrease in MCP-1 levels, a cytokine that is secreted during inflammation. In addition to the potential anti-inflammatory activity of QMC, the anti-cancer effect of the compound could also involve in a decrease in inflammatory signals, signals that are part of the proliferation of malignant neoplastic cells [7, 39-40].

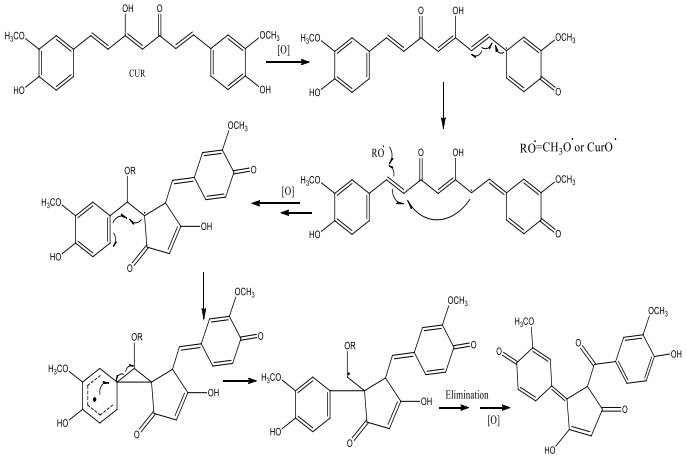

Scheme 1: Proposed mechanism of formation of QMC by oxidation of CUR.

CONCLUSION

In conclusion, QMC, a new oxidative product of CUR, has been found to be water-soluble, effective as CUR, and a relatively stable molecule, providing a better chance for curcuminoids to eventually be therapeutic agents in the clinical practice. Further experimentation remains to be done, predominantly the evaluation of its oral bioavailability and pharmacokinetics.

Conflicts of Interest

The authors declare that they have no conflict of interest.

REFERENCES

1. Goel A, Kunnumakkara AB, Aggarwal BB. Curcumin as "Curecumin": from kitchen to clinic. Biochem. Pharmacol. 2008; 75(4):787-809.
2. Hewlings SJ, Kalman DS. Curcumin: a review of its effects on human health. Foods 2017; 6(10):92.
3. Sun Y-M, Wang R-X, Yuan S-L, Lin X-J, Liu C-B. Theoretical study on the antioxidant activity of curcumin. Chin. J. Chem. 2004; 22:827-830.
4. Grynkiewicz G, Ślifirski P. Curcumin and curcuminoids in quest for medicinal status. Acta Biochim. Pol. 2012; 59(2):201-212.
5. Middleton E Jr, Kandaswami C, Theoharides TC. The effects of plant flavonoids on ammalian cells: implications for inflammation, heart disease, and cancer. Pharmacol. Rev. 2000; 52(4):673-751.
6. Weisberg SP, Leibel R, Tortoriello DV. Dietary curcumin significantly improves obesity-associated inflammation and diabetes in mouse models of diabesity. Endocrinology 2008; 149(7):3549-3558.
7. Perrone D, Ardito F, Giannatempo G, *et al.* Biological and therapeutic activities, and anticancer properties of curcumin. Exp. Ther. Med. (2015); 10(5):1615-1623.
8. Sun J, Zhao Y, Hu J. Curcumin inhibits imiquimod-induced psoriasis-like inflammation by inhibiting IL-1beta and IL-6 production in mice. PLoS One 2013; 8(6):e67078.
9. Antiga E, Bonciolini V, Volpi W, Del Bianco E, Caproni M. Oral curcumin (meriva) is effective as an adjuvant treatment and is able to reduce IL-22 serum levels in patients with psoriasis vulgaris. BioMed Res. Int. 2015; 2015:2836634.
10. Kang D, Li B, Luo L, *et al.* Curcumin shows excellent therapeutic effect on psoriasis in mouse model. Biochimie 2016; 123:73-80.
11. Priyadarsini KI. The chemistry of curcumin: from extraction to therapeutic agent. Molecules 2014; 19(12):20091-20112.
12. Tønnesen HH, Karlsen J. Studies on curcumin and curcuminoids. Z. Lebensm. Unters Forch. 1985; 180:402–404.
13. Wang YJ, Pan MH, Cheng AL, Lin LI, Ho YS, Hsieh CY, Lin JK. Stability of curcumin in buffer solutions and characterization of its degradation products. J. Pharm. Biomed. Anal. 1997; 15(12):1867-1876.
14. Tsuda T. Curcumin as a functional food-derived factor: degradation products, metabolites, bioactivity, and future perspectives. Food Funct. 2018; 9(2):705-714.
15. Shen L, Ji HF. The pharmacology of curcumin: is it the degradation products? Trends Mol. Med. 2012; 18(3):138-144.
16. Shen L, Liu C, An C *et al.* How does curcumin work with poor bioavailability? Clues from experimental and theoretical studies. Sci. Rep. 2016; 6:20872.
17. Hassaninasab A, Hashimoto Y, Tomita-Yokotani K, Kobayashi M. Discovery of the curcumin metabolic pathway involving a unique enzyme in an intestinal microorganism. Proc. Natl. Acad. Sci. USA 2011; 108(16):6615-6620.
18. Holder GM, Plummer JL, Ryan AJ. The metabolism and excretion of curcumin (1,7-bis-(4-hydroxy-3-methoxyphenyl)-1,6-heptadiene-3,5-dione) in the rat. Xenobiotica 1978; 8(12):761-768.
19. Wahlström B, Blennow G. A study on the fate of curcumin in the rat. Acta Pharmacol. Toxicol. (Copenh.) 1978; 43(2):86-92.
20. Metzler M, Pfeiffer E, Schulz SI, Dempe JS. Curcumin uptake and metabolism. Biofactors 2013; 39(1):14-20.
21. Ireson C, Orr S, Jones DJ, *et al.* Characterization of metabolites of the chemopreventive agent curcumin in human and rat hepatocytes and in the rat in vivo, and evaluation of their ability to inhibit phorbol ester-induced prostaglandin E2 production. Cancer Res. 2001; 61(3):1058-1064.
22. Griesser M, Pistis V, Suzuki T, Tejera N, Pratt DA, Schneider C. Autoxidative and cyclooxygenase-2 catalyzed transformation of the dietary chemopreventive agent curcumin. J. Biol. Chem. 2011; 286(2):1114-1124.
23. Gordon ON, Luis PB, Sintim HO Schneider C. Unraveling curcumin degradation: autoxidation proceeds through spiroepoxide and vinylether intermediates en route to the main bicyclopentadione. J. Biol. Chem. 2015; 290(8):4817-4828.
24. Schneider C, Amberg A, Feurle J, *et al.* 2-[(4"-hydroxy-3'-methoxy)-phenoxy]-4-(4"-hydroxy-3"-methoxy- phenyl)-8-hydroxy-6-oxo-3-oxabicylo[3.3.0]-7-octene: Unusual product of the soybean lipoxygenase-catalyzed oxygenation of curcumin. J. Mol. Catal. B: Enzym. 1998; 4(4):219-227.
25. Sanidad KZ, Zhu J, Wang W, Du Z, Zhang G. Effects of stable degradation products of curcumin on cancer cell proliferation and inflammation. J. Agric. Food Chem. 2016; 64(48):9189-9195.
26. Zhu J, Sanidad KZ, Sukamtoh E, Zhang G. Potential roles of chemical degradation in the biological activities of curcumin. Food Funct. 2017; 8(3):907-914.
27. Krysin AP, Genaev AM, Pokrovskii LM, *et al.* Oxidative dimerization of 2,6-Di-*tert*-butyl-4-(2-hydroxyethyl)phenol. Russ. J. Org. Chem. 2014; 50:367–370.
28. Jutooru I, Chadalapaka G, Lei P, Safe S. Inhibition of NF kappaB and pancreatic cancer cell and tumor growth by curcumin is dependent on specificity protein down-regulation. J. Biol. Chem. 2010; 285(33):25332-25344.
29. Menegon S, Columbano A, Giordano S. The Dual Roles of NRF2 in Cancer. Trends Mol. Med. 2016; 22(7):578-593.
30. Marquardt JU, Gomez-Quiroz L, Arreguin Camacho LO, *et al.* Curcumin effectively inhibits oncogenic NF-κB signaling and restrains stemness features in liver cancer. J. Hepatol. 2015; 63(3):661-669.
31. Chen B, Zhang Y, Wang Y, Rao J, Jiang X, Xu Z. Curcumin inhibits proliferation of breast cancer cells through Nrf2-mediated down-regulation of Fen1 expression. J. Steroid Biochem. Mol. Biol. 2014; 143:11-18.

32. Cho JW, Lee KS, Kim CW. Curcumin attenuates the expression of IL-1beta, IL-6, and TNF-alpha as well as cyclin E in TNF-alpha-treated HaCaT cells; NF-kappaB and MAPKs as potential upstream targets. Int. J. Mol. Med. 2007; 19(3):469-474.
33. Youn GS, Kwon DJ, Ju SM, Choi SY, Park J. Curcumin ameliorates TNF-α-induced ICAM-1 expression and subsequent THP-1 adhesiveness via the induction of heme oxygenase-1 in the HaCaT cells. BMB Rep. 2013; 46(8):410-415.
34. Kong L, Liu J, Wang J, *et al*. Icariin inhibits TNF-α/IFN-γ induced inflammatory response via inhibition of the substance P and p38-MAPK signaling pathway in human keratinocytes. Int. Immunopharmacol. 2015; 29(2):401-407.
35. Suprihatin T, Widyarti S, Rifa'I M, Rahayu S. Computational study of curcumin as antioxidant and potential inhibitor to abrogate Keap1-Nrf2 interaction. Medicinal Plants-International Journal of Phytomedicines and Related Industries 2017; 9(3):150-153.
36. Kumar A, Bora U. In silico inhibition studies of NF-κB p50 subunit by curcumin and its natural derivatives. Med. Chem. Res. 2012; 21:3281-3287.
37. Dahan A, Markovic M, Epstein S, *et al*. Phospholipid-drug conjugates as a novel oral drug targeting approach for the treatment of inflammatory bowel disease. Eur. J. Pharm. Sci. 2017; 108:78-85.
38. Ramya PVS, Guntuku L, Angapelly S, Digwal CS, Lakshmi UJ, Sigalapalli DK, Babu BN, Naidu VGM, Kamal A. Synthesis and biological evaluation of curcumin inspired imidazo [1, 2-a] pyridine analogues as tubulin polymerization inhibitors. Eur. J. Med. Chem. 2018; 143:216-231.
39. Leu TH, Maa MC. The molecular mechanisms for the antitumorigenic effect of curcumin. Curr. Med. Chem. Anticancer Agents 2002; 2(3):357-370.
40. Kunnumakkara AB, Anand P, Aggarwal BB. Curcumin inhibits proliferation, invasion, angiogenesis and metastasis of different cancers through interaction with multiple cell signaling proteins. Cancer Lett. 2008; 269(2):199-225.
41. Bar-Sela G, Epelbaum R, Schaffer M. Curcumin as an anti-cancer agent: review of the gap between basic and clinical applications. Curr. Med. Chem. 2010; 17(3):190-197.
42. Jaramillo MC, Zhang DD. The emerging role of the Nrf2-Keap1 signaling pathway in cancer. Genes Dev. 2013; 27(20):2179-2191.
43. Kwak MK, Kensler TW. Targeting NRF2 signaling for cancer chemoprevention. Toxicol. Appl. Pharmacol. 2010; 244(1):66-76.
44. Bellezza I, Mierla AL, Minelli A. Nrf2 and NF-κB and Their Concerted Modulation in Cancer Pathogenesis and Progression. Cancers (Basel) 2010; 2(2):483-497.
45. Rushworth SA, Zaitseva L, Murray MY, Shah NM, Bowles KM, MacEwan DJ. The high Nrf2 expression in human acute myeloid leukemia is driven by NF-κB and underlies its chemo-resistance. Blood 2012; 120(26):5188-5198.
46. Khurana N, Sikka SC. Targeting Crosstalk between Nrf-2, NF-κB and Androgen Receptor Signaling in Prostate Cancer. Cancers (Basel) 2018; 10(10):352.
47. Mukhopadhyay A, Bueso-Ramos C, Chatterjee D, Pantazis P, Aggarwal BB. Curcumin downregulates cell survival mechanisms in human prostate cancer cell lines. Oncogene 2001; 20(52):7597-7609.
48. Deeb D, Jiang H, Gao X, *et al*. Curcumin sensitizes prostate cancer cells to tumor necrosis factor-related apoptosis-inducing ligand/Apo2L by inhibiting nuclear factor-kappa B through suppression of Ikappa-B-alpha phosphorylation. Mol. Cancer Ther. 2004; 3(7):803-812.
49. Balogun E, Hoque M, Gong P, *et al*. Curcumin activates the haem oxygenase-1 gene via regulation of Nrf2 and the antioxidant-responsive element. Biochem. J. 2003; 371(3):887-895.
50. Taguchi K, Yamamoto M. The KEAP1-NRF2 system in cancer. Front. Oncol. 2017; 7:85.
51. Liu JY, Hu JH, Zhu QG, Li FQ, Wang J, Sun HJ. Effect of matrine on the expression of substance P receptor and inflammatory cytokines production in human skin keratinocytes and fibroblasts. Int. Immunopharmacol. 2007; 7(6):816-823.
52. Sintov AC, Yarmolinsky L, Dahan A, Ben-Shabat S. Pharmacological effects of vitamin D and its analogs: recent developments. Drug Discov. Today 2014; 19(11):1769-1774.
53. Edwards RL, Luis PB, Varuzza PV, *et al*. The anti-inflammatory activity of curcumin is mediated by its oxidative metabolites. J. Biol. Chem. 2017; 292(52):21243-21252.
54. Hashim MF, Hakamatsuka T, Ebizuka Y, Sankawa U. Reaction mechanism of oxidative rearrangement of flavanone in isoflavone biosynthesis. FEBS Lett. 1990; 271(1-2):219-222.
55. Kasi PD, Tamilselvam R, Skalicka-Woźniak K, *et al*. Molecular targets of curcumin for cancer therapy: an updated review. Tumour Biol. 2016; 37(10):13017-13028.
56. Mishra A, Kumar R, Tyagi A, *et al*. Curcumin modulates cellular AP-1, NF-kB, and HPV16 E6 proteins in oral cancer. Ecancermedicalscience 2015; 9:525.

HOW TO CITE THIS ARTICLE

Sinai T, Singh B, Sintov AC, Shabat SB. Synthesis, Isolation, and Biological Evaluation of a New Active Quinone Methide Derived Curcuminoid. J Phytopharmacol 2021; 10(1):48-55.